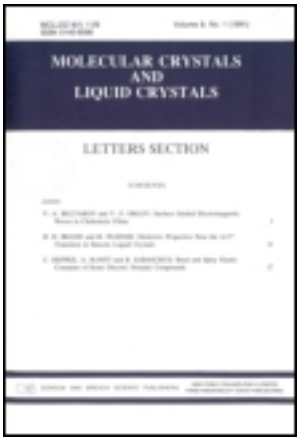

Molecular Crystals and Liquid Crystals
Publication details, including instructions for authors and subscription information:
http://www.tandfonline.com/loi/gmcl20

Morphological Control of Gold Nanoparticle Aggregates via Photoisomerization of Azobenzene Liquid Crystals

Kaori Fujisawa [a], Asuna Kuranari [b], Koji Ota [b] & Osamu Tsutsumi [b]
[a] Ritsumeikan Global Innovation Research Organization (R-GIRO), Ritsumeikan University, 1-1-1 Nojihigashi, Kusatsu, 525-8577, Japan
[b] Department of Applied Chemistry, Ritsumeikan University, 1-1-1 Nojihigashi, Kusatsu, 525-8577, Japan
Published online: 16 Dec 2013.

To cite this article: Kaori Fujisawa, Asuna Kuranari, Koji Ota & Osamu Tsutsumi (2013) Morphological Control of Gold Nanoparticle Aggregates via Photoisomerization of Azobenzene Liquid Crystals, Molecular Crystals and Liquid Crystals, 583:1, 21-28, DOI: 10.1080/15421406.2013.843817

To link to this article: http://dx.doi.org/10.1080/15421406.2013.843817

Mol. Cryst. Liq. Cryst., Vol. 583: pp. 21–28, 2013

ISSN: 1542-1406 print/1563-5287 online
DOI: 10.1080/15421406.2013.843817

Taylor & Francis
Taylor & Francis Group

Morphological Control of Gold Nanoparticle Aggregates via Photoisomerization of Azobenzene Liquid Crystals

KAORI FUJISAWA,[1] ASUNA KURANARI,[2] KOJI OTA,[2] AND OSAMU TSUTSUMI[2,*]

[1]Ritsumeikan Global Innovation Research Organization (R-GIRO), Ritsumeikan University, 1-1-1 Nojihigashi, Kusatsu 525-8577, Japan
[2]Department of Applied Chemistry, Ritsumeikan University, 1-1-1 Nojihigashi, Kusatsu 525-8577, Japan

Gold nanoparticles having a monolayer of azobenzene liquid crystals (LCs) were synthesized and their aggregation structures on solid surfaces were observed. The gold nanoparticles formed a single-particle layer on bare mica and mica with a polyimide layer. We demonstrated that the morphology of the gold nanoparticle aggregates could be controlled by UV light irradiation at 366 nm; the mass transfer of gold nanoparticles from the exposed area to the nonexposed area was induced by the isomerization of azobenzene LC molecules.

Keywords Azobenzene; gold nanoparticle; liquid crystal; photochromism; self-assembly

1. Introduction

Monolayer-protected metal nanoparticles have attracted great interest because they show unique physical and chemical properties afforded by quantum-size effects [1]. Therefore, such nanoparticles are expected to be applicable as novel materials for electronic, photonic, and magnetic devices [1,2]. For device applications, the nanoparticles should be arranged in an ordered structure; in this regard, 1-, 2- and 3-dimensional arrangements of various metal nanoparticles have been reported [3].

Liquid crystals (LCs) are materials that show a long-range order in molecular alignment, cooperative effects, and anisotropies in optical, electronic, and magnetic properties [4]. It has been reported that metal nanoparticles can be spatially arranged via the self-assembly of LC molecules [5]. We may consider that self-assembled nanoparticle structures can be controlled by external stimuli. This is because owing to their fluidity, LCs can respond to external stimuli such as electric fields and light.

Azobenzene derivatives are well-known photochromic chromophores and show reversible *trans-cis* isomerization upon irradiation [6,7]. Some azobenzene derivatives are also known as mesogens, and many types of azobenzene LCs have been developed so far

*Address correspondence to Prof. Osamu Tsutsumi, Department of Applied Chemistry, College of Life Sciences, Ritsumeikan University, 1-1-1 Nojihigashi, Kusatsu 525-8577, Japan. Tel.: (+81) 77-561-5966; Fax: (+81) 77-561-2659. E-mail: tsutsumi@sk.ritsumei.ac.jp

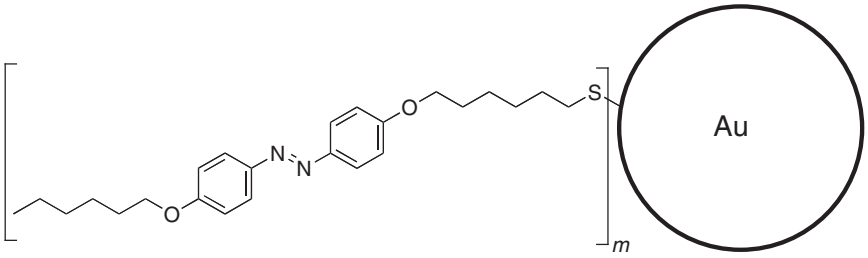

Figure 1. Structure of gold nanoparticles (Au-Azo) used in this study.

[7,8]. It has been demonstrated that the LC phase structure and the direction of the molecular alignment of LCs can be controlled by light. This could be attributed to the fact that the molecular shape, liquid crystallinity, and dipole moment of azobenzene molecules are changed by photoisomerization; in other words, azobenzene derivatives can act as photoresponsive LCs. Therefore, when azobenzene LCs are introduced onto the surface of metal nanoparticles, we can expect to control the aggregation structures of the nanoparticles by light. In this study, we synthesized gold nanoparticles with azobenzene mesogens on their surface and observed the changes induced by photoirradiation in morphological structures of gold nanoparticle aggregates.

2. Experimental

Materials

The structure of the gold nanoparticles used in this study is shown in Fig. 1. The azobenzene LC molecules were linked with the gold nanoparticles through an Au–S covalent bond. The resulting structure is denoted hereafter as Au-Azo. Gold nanoparticles were prepared through the modification of a previously reported method [9]. The structures of the azobenzene ligands and gold nanoparticles were confirmed by NMR and transmission electron microscopy (TEM: JEOL JEM-3100FEF, 300 kV), respectively. The size and size distribution of the gold nanoparticles were determined by TEM.

Characterization of Gold Nanoparticles

LC behaviors were examined using a polarizing microscope (Olympus, Model BX51) equipped with a hot stage (Instec HCS302 hot stage and mK1000 controller). The thermodynamic properties of the material were determined by differential scanning calorimetry (DSC, Perkin Elmer Diamond DSC) at heating and cooling rates of 1.0°C/min. At least three scans were performed for each sample to check reproducibility. Thermogravimetric (TG) analysis was performed using DTG-60AH (Shimadzu) at a heating rate of 10°C/min to determine the weight ratio of the metal and the organic compound, as well as the decomposition temperature.

Gold Nanoparticle Aggregates

The structures of the gold nanoparticle aggregates were recorded by atomic force microscopy (AFM). The AFM images of gold nanoparticles on a mica substrate treated with a

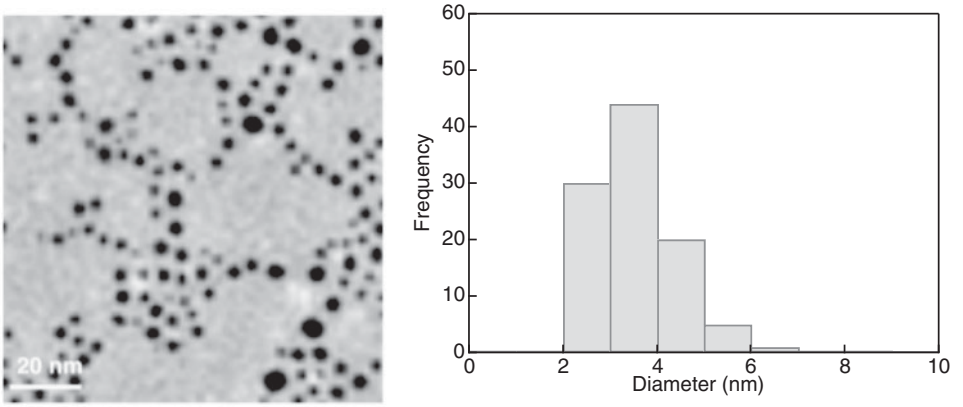

Figure 2. (a) TEM image of nanoparticles; (b) histogram representing the diameter of nanoparticles.

polyimide alignment layer were observed. The mica substrates were spin-coated with a solution of 2.5 wt% polyamic acid in a mixture of *N*-methylpyrrolidone and γ-butyrolactone (1:2 v/v). The spinning velocity was 300 rpm (5 s^{-1}) for the first 3 s and 3,000 rpm (50 s^{-1}) for next 30 s. The spin-coated substrate was then baked in an oven at 100°C for 1 h and at 250°C for 2 h to obtain a thin layer of polyimide.

The gold nanoparticles were dissolved in dichloromethane (0.1 g/L) and 10 μL of the resultant solution was cast onto the desired substrate. After the solvent was slowly evaporated at room temperature (15°C), the aggregation structures of the nanoparticles were observed by AFM. For the photochemical control of the aggregation structures, the nanoparticles on the substrate were irradiated with UV light (366 nm, 52 J/cm^2) through a photomask during the solvent-evaporation process.

3. Results and Discussion

Characterization of Au-Azo

Figure 2 shows a typical TEM image of Au-Azo. From the TEM image, we estimated the size of the gold nanoparticles in Au-Azo. The figure also shows the histogram representing the diameter of the nanoparticles. The histogram indicates that the diameter had a unimodal distribution; the estimated average diameter was 3.5 $\pm$ 1.1 nm.

The TG analysis of Au-Azo indicated a 28% weight loss upon heating the sample up to 550°C. This result means that Au-Azo contained 28 wt% of azobenzene LC molecules on average. From the diameter of the gold nanoparticles and the weight percentage of azobenzene LCs, we can estimate the average number of gold atoms, m_{Au}, and the average number of azobenzene LC molecules, m_{Azo}, comprising Au-Azo, by using Eqs. 1 and 2 [10].

$$m_{Au} = 4\pi N_A r^3 / 3V_{Au} \tag{1}$$

$$m_{Azo} = (m \times AW_{Au} \times wt\%_{Azo})/(MW_{Azo} \times wt\%_{Au}) \tag{2}$$

where N_A is the Avogadro constant, r is the average radius of the nanoparticles, V_{Au} is the molar volume of gold (10.2 cm^3 mol^{-1}), AW_{Au} and MW_{Azo} are the atomic weight of

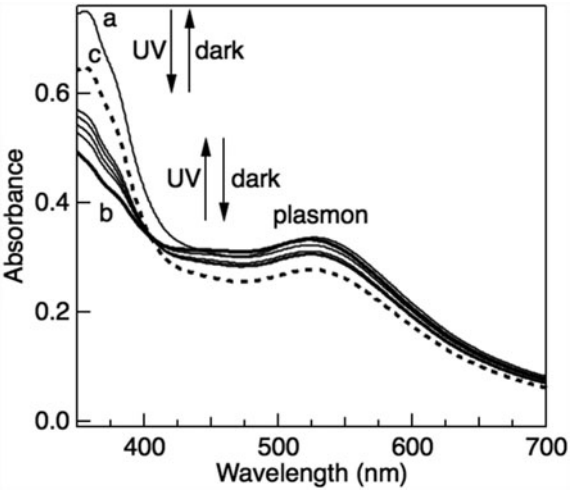

Figure 3. UV-vis absorption spectra of Au-Azo in dichloromethane (38 mg/L): (a) as-prepared solution; (b) just after irradiation with UV light at 366 nm; and (c) sample kept in the dark at room temperature for 18 h after irradiation.

gold and the molecular weight of azobenzene LC, respectively, and $wt\%_{\mathrm{Azo}}$ and $wt\%_{\mathrm{Au}}$ are the weight percentages of azobenzene LC and gold, respectively. From Eqs. 1 and 2, we obtained $m_{\mathrm{Au}} = 1.3 \times 10^3$ and $m_{\mathrm{Azo}} = 96$, respectively.

From the results of polarizing microscopy and DSC, it was confirmed that the free azobenzene ligand showed an LC phase. The DSC thermogram of Au-Azo exhibited several endothermic and exothermic peaks upon heating and cooling, but those peaks were not reproducible on repeated runs. We conclude from this result that not only phase transitions of Au-Azo took place but also its thermal decomposition occurred during the heating and cooling processes. The TEM observation of Au-Azo after heating up to 80°C showed the presence of many large particles with diameters of more than 10 nm, which we considered to have resulted from the coalescence of gold nanoparticles upon heating.

Photoisomerization Behavior of Au-Azo

Figure 3 shows the UV-vis absorption spectra of Au-Azo in a dichloromethane solution. The absorption spectrum of the as-prepared solution exhibited absorption maxima at around 360 nm and 450 nm, which can be attributed to the π–π^* absorption and n–π^* absorption, respectively. In addition, a broad absorption band also appeared at around 550 nm. It is known that nanometer-scale gold particles show an absorption band with an absorption maximum of >500 nm [1], and thus, this absorption band can be assigned to the surface plasmon resonance of the gold nanoparticles.

From UV-vis absorption spectroscopy, we confirmed that UV irradiation of the Au-Azo solution at 366 nm induced the *trans-cis* photoisomerization of the azobenzene moiety, even on the surface of the gold nanoparticles. Furthermore, when the irradiated solution was kept in the dark, thermal back-isomerization occurred. Thus, we can conclude that the azobenzene molecules immobilized on the surface of the gold nanoparticles show a reversible photochromic reaction, as is the case with free azobenzene molecules in solutions.

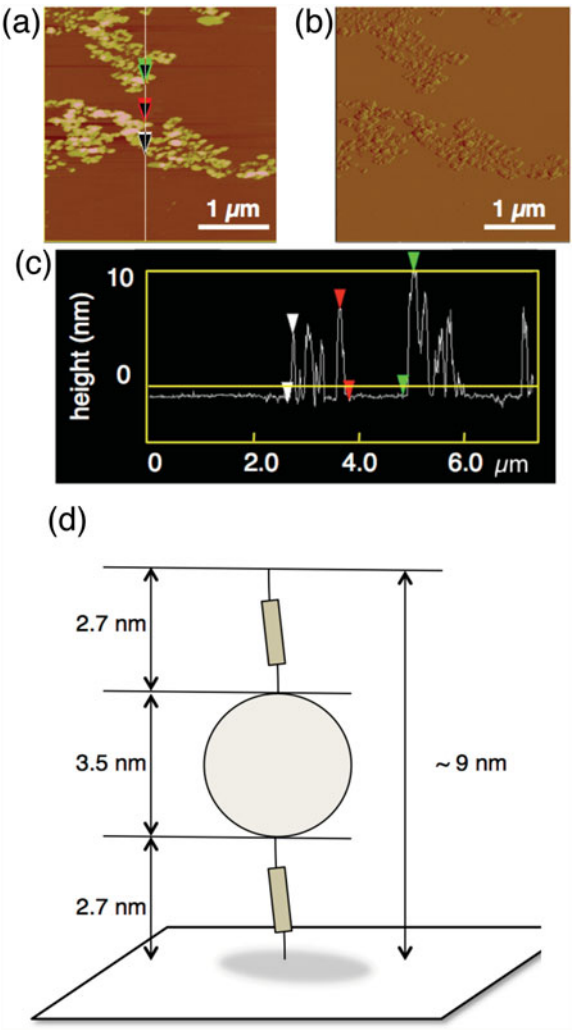

Figure 4. AFM images of Au-Azo on a bare mica substrate: (a) topographic image (7.4 μm $\times$ 7.4 μm); (b) corresponding deflection image (error signal); and (c) cross-sectional image. (d) Schematic illustration of Au-Azo on bare mica surface.

Aggregation Structures of Au-Azo

Using AFM, we observed the aggregation structures of the gold nanoparticles on various solid substrates. On a mica substrate, Au-Azo showed a random aggregation structure about 9-nm high (Fig. 4). The length of the azobenzene LC molecule was estimated to be 2.7 nm through density functional theory (DFT) calculations [B3LYP/6-31G(d,p) level], so that the diameter of Au-Azo nanoparticles is ~9 nm [Fig. 4(d)]. The height of Au-Azo on the mica substrate observed with AFM is in agreement with its diameter. This means that the Au-Azo nanoparticles formed a single layer on the mica surface.

Figure 5 shows AFM images of Au-Azo on the polyimide-coated mica substrate. On this substrate, Au-Azo was more dispersed and primarily formed random aggregations. However, some linear aggregations were also observed on the polyimide layer. At present,

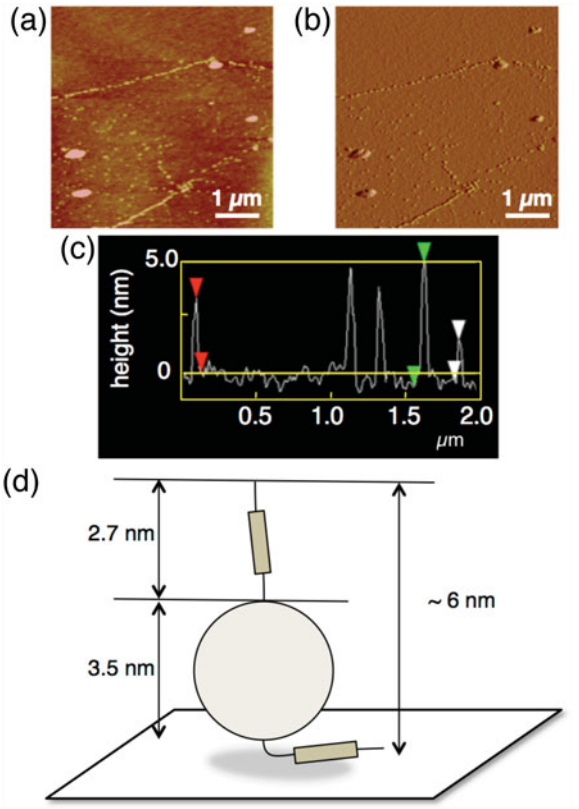

Figure 5. AFM images of Au-Azo on a polyimide-coated mica substrate: (a) topographic image (5 μm $\times$ 5 μm); (b) corresponding deflection image (error signal); and (c) cross-sectional image. (d) Schematic illustration of Au-Azo on polyimide layer.

the reason for the formation of the linear aggregation is not clear. The height of the nanoparticles was about 5 nm, implying that Au-Azo formed a single nanoparticle layer on the polyimide layer as well. Generally, thin films of polyimide are used as LC alignment layers for LC devices because this polymer has a high affinity with LC molecules and can therefore control the molecular alignment of LCs [11]. Thus, we consider that the molecular long axis of an azobenzene LC molecule in contact with the polyimide layer was parallel to the surface of the polyimide layer [Fig. 5(d)] but perpendicular to the surface on the bare mica substrate [Fig. 4(d)]. This difference in alignment could be attributed to the hydrophilicity of the mica surface. Consequently, the height of the Au-Azo single nanoparticle layer on the polyimide (5 nm) was lower than that on the bare mica surface (9 nm).

Photochemical Control of Morphology

Figure 6 shows the AFM images of Au-Azo on the polyimide-coated mica substrate, obtained after irradiation with UV light at 366 nm through a photomask during the drying process under a saturated dichloromethane atmosphere (Fig. 6). As seen in the figure, Au-Azo was much more sparsely dispersed in the exposed area; it was actually difficult to spot

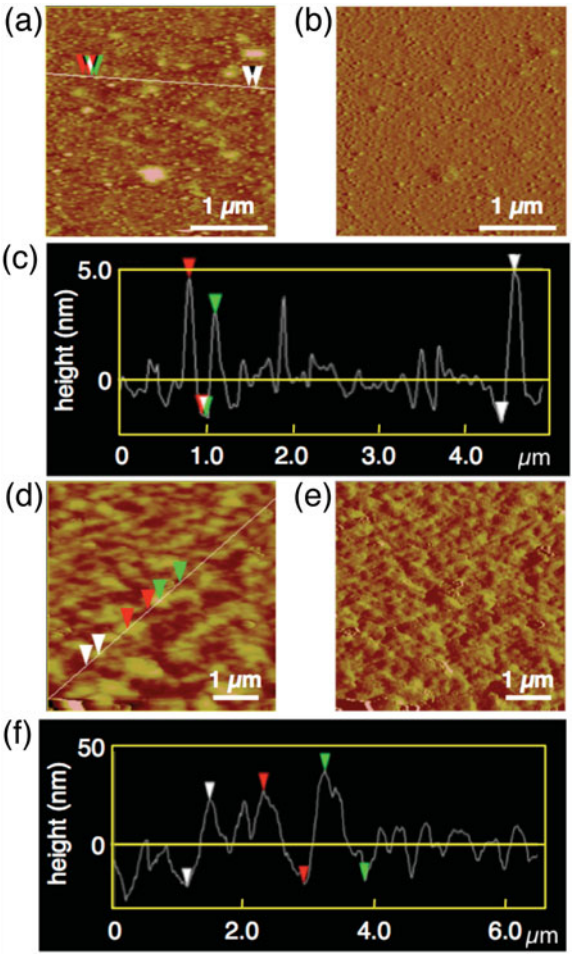

Figure 6. AFM images of Au-Azo prepared on a polyimide-coated mica substrate, after exposure to UV light at 366 nm through a photomask: (a) topographic image of the exposed area (3 μm × 3 μm); (b) corresponding deflection image (error signal); (c) cross-sectional image of (a); (d) topographic image of the non-exposed area (5 μm × 5 μm); (e) corresponding deflection image (error signal); and (f) cross-sectional image of (d).

nanoparticles in the AFM images because they were too rare in this area [Figs. 6(a)–(c)]. However, in the nonexposed area, many nanoparticles were present, and they formed large aggregations with heights of about 50 nm [Figs. 6(d)–(f)]. The results suggest that the nanoparticles moved from the exposed area to the nonexposed area upon UV irradiation at 366 nm.

It is known that in azobenzene polymer films, mass transfer is induced by photoirradiation, i.e., the azobenzene polymer molecules move from an exposed area to a nonexposed area. For example, when the azobenzene polymer films are exposed to a bright-and-dark interference pattern created by two coherent laser beams, the molecules move from the bright areas to the dark areas, as shown by the interference pattern. As a result, relief structures are formed on the surface of the films. This phenomenon is known as the surface relief grating (SRG) formation, but the mechanism behind this phenomenon is not yet clear

[7]. We consider that the same phenomenon is observed in the gold nanoparticles with azobenzene LC molecules.

4. Conclusion

In this study, gold nanoparticles with azobenzene LC molecules were synthesized. We demonstrated that photoirradiation caused a mass transfer of gold nanoparticles from the exposed area to the nonexposed area and that the morphology of gold nanoparticle aggregates can be controlled by light. The phenomenon observed in this study suggests that gold nanoparticle patterns can be easily formed by light. In addition, since the gold nanoparticles coalesce upon heating, we can expect to construct nanoscale gold wirings for integrated circuits without using the photolithography technique.

Acknowledgments

This work was partly supported by a Grant-in-Aid for Scientific Research (C) (24550217) (O.T.) from the Japan Society for Promotion of Science (JSPS), the A-STEP (AS231Z04286D) (O.T.) from the Japan Science and Technology Agency (JST), and the MEXT-Supported Program for the Strategic Research Foundation at Private Universities, 2012–2016. Moreover, the research was technically supported by the Kyoto Advanced Nanotechnology Network (Nara Institute of Science and Technology).

References

[1] (a) Raether, H. (1998). *Surface Plasmons*, Springr-Verlag: Berlin. (b) Krenn, J. R. et al. (1999). *Physical Review B*, *60*, 5029–5033.
[2] Daniel, M. C., & Astruc, D. (2004). *Chem. Rev.*, *104*, 293–346.
[3] (a) Keng, P. Y., Shim, I., Korth, B. D., Douglas, J. F., & Pyun, J. (2007). *ACS Nano*, *1*, 279–292. (b) Markovich, N., Volinsky, R., & Jelinek, R. (2009). *J. Am. Chem. Soc*., *131*, 2430–2431. (c) Sardar, R., Funston, A. M., Mulvaney, P., & Murray, R. W. (2009). *Langmuir*, *25*, 13840–13851. (d) Satake, A., Fujita, M., Kurimoto, Y., & Kobuke, Y. (2009). *Chem. Commun*., 1231–1233. (e) Weizmann, Y., Chenoweth, D. M., & Swager, T. M. (2010). *J. Am. Chem. Soc*., *132*, 14009–14011.
[4] Khoo, I.-C. (2007). *Liquid Crystals*, Wiley-Interscience: Hobonken, NJ.
[5] (a) Kanayama, N., Tsutsumi, O., Kanazawa, A., & Ikeda, T. (2001). *Chem. Commun*., 2640–2641. (b) In, I., Jun, Y. W., Kim, Y. J., & Kim, S. Y. (2005). *Chem. Commun*., 800–801. (c) Shen, Z., Yamada, M., & Miyake, M. (2007). *J. Am. Chem. Soc*., *129*, 14271–14280.
[6] Bandara, H. M. D., & Burdette, S. C. (2012). *Chem. Soc. Rev.*, *41*, 1809–1825.
[7] (a) Natansohn, A., & Rochon, P. (2002). *Chem. Rev.*, *102*, 4139–4176. (b) Matharu, A. S., Jeeva, S. & Ramanujam, P. S. (2007). *Chem. Soc. Rev.*, *36*, 1868–1880.
[8] Ikeda, T., & Tsutsumi, O. (1995). *Science*, *268*, 1873–1875.
[9] (a) Brust, M., Walker, M., Bethell, D., Schiffrin, D. J., & Whyman, R. (1994). *Chem. Commun*., 801–802. (b) Tsutsumi, O. *et al*. (2011). *Mol. Cryst. Liq. Cryst*., *550*, 105–111.
[10] Hou, W., Dasog, M., & Scott, R. W. J. (2009). *Langmuir*, *25*, 12954–12961.
[11] Wang, Y. *et al*. (1998). *J. Appl. Phys*., *84*, 181–188.